Noninvasive Imaging of Islet Transplants with ^{111}In-Exendin-3 SPECT/CT

Inge van der Kroon*, Karolina Andralojc*, Stefanie M.A. Willekens, Desirée Bos, Lieke Joosten, Otto C. Boerman, Maarten Brom, and Martin Gotthardt

Department of Radiology and Nuclear Medicine, Radboud University Medical Center, Nijmegen, the Netherlands

Islet transplantation is a promising treatment for type 1 diabetic patients. However, there is acute as well as chronic loss of islets after transplantation. A noninvasive imaging method that could monitor islet mass might help to improve transplantation outcomes. In this study, islets were visualized after transplantation in a rat model with a dedicated small-animal SPECT scanner by targeting the glucagonlike peptide-1 receptor (GLP-1R), specifically expressed on β-cells, with ^{111}In-labeled exendin-3. **Methods:** Targeting of ^{111}In-exendin-3 to GLP-1R was tested in vitro on isolated islets of WAG/Rij rats. For in vivo evaluation, 400 or 800 islets were transplanted into the calf muscle of WAG/Rij rats (6–8 wk old). Four weeks after transplantation, SPECT/CT images were acquired 1 h after injection of ^{111}In-labeled exendin-3. After SPECT acquisition, the muscles containing the transplant were analyzed immunohistochemically and autoradiographically. **Results:** The binding assay, performed on isolated islets, showed a linear correlation between the number of islets and ^{111}In-exendin-3 accumulation (Pearson $r = 0.98$). In vivo, a 1.70 ± 0.44-fold difference in tracer uptake between 400 and 800 transplanted islets was observed. Ex vivo analysis of the islet transplant showed colocalization of tracer accumulation on autoradiography, with insulin-positive cells and GLP-1R expression on immunohistochemistry. **Conclusion:** ^{111}In-exendin-3 accumulates specifically in the β-cells after islet transplantation and is a promising tracer for noninvasive monitoring of the islet mass.

Key Words: exendin-3; GLP-1R; islet transplantation; SPECT; islet imaging

For type 1 diabetic patients with poor glycemic control, pancreatic islet transplantation is a promising but still experimental treatment. The standard transplantation procedure is infusion of pancreatic islets in the portal vein, where islets are trapped in the sinusoidal capillaries of the liver. Most patients become insulin-independent for more than 1 y after transplantation. However, insulin independency drops to approximately 10% 5 y after transplantation (1). Even though these insulin-dependent patients still profit from this treatment because instability of blood glucose levels and risk of hypoglycemia are reduced, further improvement of transplant survival and islet function is warranted, especially in view of the side effects of the immunosuppressive treatment that is required to prevent rejection of the transplanted islets (1–3).

Current methods of monitoring islets after transplantation, such as measurement of hemoglobin A_{1C}, C-peptide, and insulin levels, provide only functional information and cannot accurately predict the number of surviving islets. Medical imaging methods may offer the possibility of monitoring the number of surviving islets after transplantation, potentially providing information (complementary to functional capacity) about the effect of interventions on transplantation outcome. This information might help to further improve this new therapeutic approach in order to achieve longer-lasting insulin independency.

Numerous studies have investigated the feasibility of imaging transplanted islets noninvasively. Islets have been transfected to express luciferase (4), and islets from transgenic animals expressing luciferase have been used (5). Although feasibility has been proven in preclinical transplantation models, these methods require transfection of β-cells or the use of transgenic animals and are therefore relatively difficult to translate to humans. In several studies, pancreatic islets prelabeled with iron oxide contrast agents were transplanted, allowing monitoring with MRI (6,7). These methods can show the presence of islets, but it remains a matter of debate to which degree the presence of iron oxide contrast agents represents viable and functional islets. Determination of the relation between viable β-cell mass and β-cell function might therefore be difficult to achieve.

Transplanted islets also have been visualized using tracers targeting receptors specifically expressed on β-cells in the islets, such as the glucagonlike peptide-1 receptor (GLP-1R) (8). Wu et al. (9) have demonstrated the feasibility of visualizing islets transplanted into the liver by targeting GLP-1R by PET with radiolabeled exendin-4. Using a tracer to target a receptor specifically expressed on β-cells allows serial imaging in vivo. To fully exploit the potential of this imaging method, quantification of true β-cell mass in islet transplants should be established for validation of in vivo imaging results.

Establishing and characterizing quantitative β-cell imaging by targeting of GLP-1R requires a simple transplantation model that allows accurate evaluation of tracer accumulation and histologic verification of imaging findings. A suitable location for islet transplantation is muscle. Muscle is already used in clinical islet transplantation (10–13), and since all islets are clustered in one location, tracer uptake can be determined by quantitative analysis of PET and SPECT images, and islet survival can easily be verified histologically.

In this study, we demonstrated the feasibility of noninvasive in vivo imaging of different numbers of islets, transplanted into the calf muscle, by targeting of GLP-1R with ^{111}In-labeled exendin-3.

MATERIALS AND METHODS

Radiolabeling

[Lys40(DTPA)]exendin-3 (Peptides Specialty Laboratories) (Fig. 1) (referred to as exendin-3 in the remainder of the text) was radiolabeled as described previously (14). Briefly, 150 MBq of ^{111}InCl$_3$ were added to 1 μg of exendin-3 dissolved in 0.1 M 2-(N-morpholino)ethanesulfonic acid (MES), pH 5.5 (Sigma Aldrich), and incubated for 20 min at room temperature. After incubation, ethylenediaminetetraacetic acid (Sigma Aldrich) and polysorbate 80 (Sigma Aldrich) were added to a final concentration of 5 mM and 0.1%, respectively. The radiochemical purity of ^{111}In-exendin-3 was determined by instant thin-layer chromatography–silica gel (Agilent Technologies), using 0.1 M NH$_4$Ac (Sigma Aldrich) in 0.1 M ethylenediaminetetraacetic acid, pH 5.5. The reaction mixture was purified by solid-phase extraction using a hydrophilic–lipophilic balance cartridge (30 mg, Oasis; Waters) to remove unlabeled ^{111}In. The cartridge was activated with 1 mL of ethanol, washed with 2 mL of water, and conditioned with 1 mL of 0.1 M MES, pH 5.5. Subsequently, the labeling mixture was loaded onto the cartridge and washed with 1 mL of 0.1 M MES and 2 mL of water. ^{111}In-exendin-3 was eluted from the cartridge with 200 μL of 100% ethanol. For injection, the purified labeling solution was diluted in 0.5% phosphate-buffered saline/bovine serum albumin (w/v) to obtain a final ethanol concentration of less than 10%.

Animals

Six- to 8-wk-old female WAG/Rij rats were purchased from Charles River Laboratories. WAG/Rij rats were used both as islet donor and as recipient. The animal experiments were approved by the animal welfare committee of the Radboud University Nijmegen.

Islet Isolation

Pancreatic islets were isolated from female WAG/Rij rats by collagenase digestion. The rats were euthanized by CO$_2$/O$_2$ suffocation, the abdominal cavity was opened, and a canula was placed in the common bile duct. The pancreas was perfused with 8 mL of RPMI medium R0883 (Gibco/BRL Thermo Fisher Scientific) containing collagenase type V (1 mg/mL; Sigma Aldrich). Subsequently, the pancreas was dissected and kept in ice-cold RPMI containing collagenase until digestion. The pancreata were digested for 11.5 min at 37°C. Digestion was stopped by addition of complete RPMI medium (RPMI medium supplemented with 10% fetal calf serum [HyClone; Celbio], 2 mM L-glutamine [Sigma Aldrich], and penicillin and streptomycin [100 U/mL; Sigma Aldrich]). The digested tissue was washed twice in complete RPMI medium (2 min at 210g) and passed through a 500-μm mesh. Subsequently, the islets were purified on a discontinuous Ficoll gradient (densities of 1.108, 1.096, and 1.037 g/mL; Cellgro [Mediatech Inc.]) by centrifugation at 625g for 16 min (without brake). The islets were collected from the interface of the second and third layers. Finally, the remaining Ficoll was removed by washing twice with complete RPMI medium (2 min at 210g). The purified islets were cultured overnight at 37°C with 5% CO$_2$ in complete RPMI medium. Both islet viability and islet purity exceeded 90% after the isolation procedure.

In Vitro Function Assay

Islet function after isolation was assessed by a static glucose incubation assay. After isolation and overnight recovery, islets were collected, counted, and resuspended in complete RPMI. Islets were seeded in a 24-well plate (Corning Inc.) at 30 islets per well (n = 5) and preincubated for 1 h (37°C, 5% CO$_2$) in 600 μL of Krebs buffer (115 mM NaCl, 24 mM NaHCO$_3$, 5 mM KCl, 2.2 mM CaCl$_2$, 1 mM MgCl$_2$, 20 mM C$_8$H$_{18}$N$_2$O$_4$S, and 0.2% bovine serum albumin [Sigma Aldrich]) supplemented with 1.67 mM D-glucose (Sigma Aldrich). After 1 h, the incubation buffer was replaced by 600 μL of fresh Krebs buffer supplemented with 1.67 mM D-glucose. Subsequently, islets were incubated in Krebs buffer supplemented with 16.7 mM D-glucose and 1.67 mM D-glucose, 1 h for both conditions. After each incubation step, the supernatant was collected and samples were stored at −20°C until insulin determination by an insulin enzyme-linked immunosorbent assay (Mercodia AB), performed according to the manufacturer's protocol.

In Vitro Binding Assay

After overnight recovery, islets were collected, counted, and resuspended in complete RPMI. After transwell saturation, using binding buffer (RPMI containing 0.5% bovine serum albumin [v/w]), islets were transferred to 24-well transwell plates (50, 100, 200, or 400 islets per transwell, n = 3 per condition) (Corning Inc.) and incubated in 500 μL of Krebs buffer for 30 min at 37°C. Subsequently, islets were washed with 500 μL of binding buffer and approximately 2 kBq of ^{111}In-exendin-3 were added, followed by incubation for 4 h at 37°C. To determine whether the binding was GLP-1R–mediated, 1 μg of unlabeled exendin-3 was added together with the radiolabeled exendin-3 in separate wells (n = 3 per condition). After incubation, islets were washed 5 times using binding buffer and islet-associated radioactivity was measured in a well-type γ-counter (Wallac 1480 Wizard; Perkin Elmer).

Transplantation

After overnight recovery, isolated islets were collected, spun down at 15g for 2 min, and resuspended in RPMI without fetal calf serum. Recipient rats were anesthetized with isoflurane (induction, 4%–5%; maintenance, 1.5%–2% in 50% O$_2$ and 50% air) (Abbott Laboratories), and the right hind leg was shaved and disinfected with povidone–iodine (Meda Pharma B.V.) before islet inoculation. Islets were aspirated into a catheter line and infused manually in the calf muscle at low speed (injected volume, 100 ± 10 μL) using a syringe (Hamilton Co.). Rats were transplanted with either 400 (n = 6) or 800 (n = 6) islets.

SPECT Acquisition and Biodistribution

Four weeks after transplantation, rats were injected with 15 ± 0.4 MBq of ^{111}In-exendin-3 via the tail vein (peptide dose, 0.1 μg in 200 μL of phosphate-buffered saline, 0.5% bovine serum albumin). One hour after injection of the radiolabeled exendin-3, rats were anesthetized with isoflurane (induction, 4%–5%; maintenance, 1.5%–2% in O$_2$ and air) and SPECT/CT was acquired using a dedicated small-animal SPECT/CT scanner (U-SPECT-II; MILabs). SPECT images were acquired with a 1.0-mm
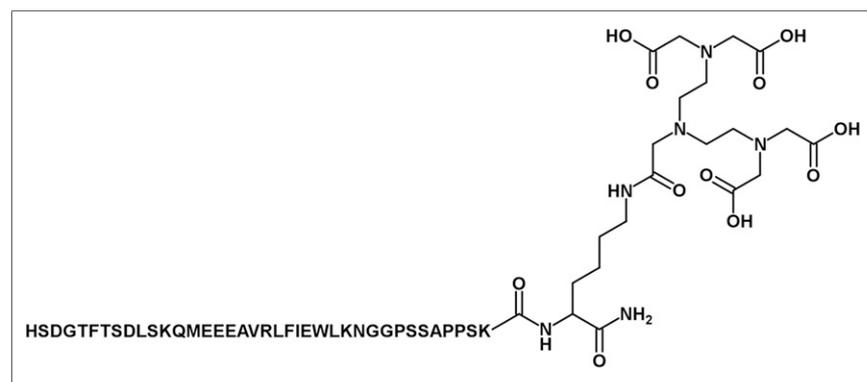

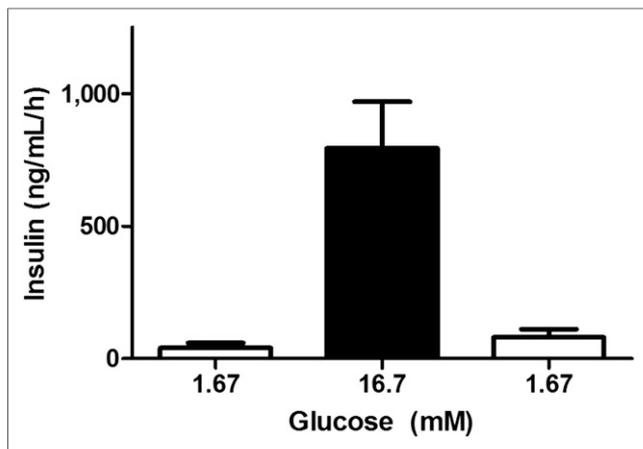**FIGURE 1.** Chemical structure of [Lys40(DTPA)]exendin-3.

FIGURE 2. Insulin release of isolated WAG/Rij islets at low (1.67 mM) and high (16.7 mM) glucose concentrations. Insulin release is expressed as ng/mL/h.

pinhole general-purpose rat and mouse collimator, 36 bed positions, and a total acquisition time of 50 min. CT images were acquired for anatomic information (65 kV, 615 μA, 1 bed position, 160-μm spatial resolution).

After the SPECT/CT acquisition (2 h after injection), rats were euthanized by CO_2/O_2 suffocation and the muscle containing the transplant, as well as other relevant tissues, were dissected, weighed, and measured in a γ-counter (Wallac 1480 Wizard). Muscles were fixed in 4% formalin (w/v).

SPECT Reconstruction and Quantitative SPECT Analysis

The SPECT images were reconstructed using the U-SPECT software (U-SPECT-Rec; MILabs) with the following settings: ordered-subsets expectation maximization, 1 iteration, 16 subsets, and a voxel size of 0.75 mm³.

Uptake of ^{111}In-exendin-3 in the transplant was quantified using Inveon Reconstruction Workplace (Siemens Healthcare). A volume of interest was placed over the transplant. Total voxel intensity in the islet transplant was corrected for the background by subtracting the background signal in the contralateral control muscle using an identical volume of interest and the injected activity.

Immunohistochemical Analysis

The formalin-fixed muscle containing the transplant was dehydrated and embedded in paraffin. Four-micrometer sections were cut and stained with hematoxylin and eosin for localization of the transplant. Consecutive sections were stained for the presence of insulin, as described previously (15), and for the presence of GLP-1R.

The GLP-1R staining was performed as follows: antigen retrieval was performed in 10 mM sodium citrate, pH 6.0, for 10 min at 99°C. Subsequently, sections were incubated for 10 min with 3% H_2O_2 in phosphate-buffered saline at room temperature in the dark, to block endogenous peroxidase activity. Nonspecific binding was blocked by incubation for 30 min with 5% swine serum. The primary anti-GLP-1R antibody (ab39072; Abcam) was diluted in phosphate-buffered saline, 1% bovine serum albumin (1:1,000). Primary antibody incubation for 90 min was followed by incubation with swine-antirabbit peroxidase (1:100) (p0271; DAKO). Finally, Bright-DAB (BS04500; Immunologic BV) was used to visualize peroxidase activity. Microautoradiography to visualize tracer accumulation was performed on 4-μm sections as described by Brom et al. (15).

Sections stained for insulin and GLP-1R were analyzed using a DM5000 microscope (Leica), and color images were obtained with a camera (Evolution MP [Leica], using AxioVision software, version 4.4 [Zeiss]). To determine transplant volume, the insulin-positive area of the transplant per section was multiplied by the intersection distance. Three animals were excluded from the analysis because no transplant was found immunohistochemically.

Statistical Analysis

All mean values are expressed as mean ± SD. Statistical analysis was performed using the unpaired 2-tailed t test, and Pearson correlation coefficients were calculated using Prism (version 5.03; GraphPad Software, Inc.). The level of significance was set at a P value of less than 0.05.

RESULTS

Radiolabeling

Exendin-3 was labeled with ^{111}In with a specific activity of 700 GBq/μmol. Radiochemical purity was more than 99% as determined by instant thin-layer chromatography.

In Vitro Function Assay

The results of the in vitro islet function assay are summarized in Figure 2. Islets responded to high glucose stimulation with an increase in insulin production from 41.1 ± 18.6 to 792 ± 176 ng/mL/h. After high glucose stimulation, insulin levels decreased to basal levels when incubated in low-glucose buffer: 80.3 ± 31.4 ng/mL/h, indicating normal function. The stimulation index, defined as the ratio of stimulated to basal insulin secretion, was 10.4 ± 1.98 ($n = 5$).

In Vitro Binding of ^{111}In-Exendin-3 to Isolated Islets

Figure 3 shows the binding of ^{111}In-exendin-3 to rat islets in vitro. After 4 h, 31 ± 3.6 amol of the added 1.28 fmol of ^{111}In-exendin-3 accumulated in 50 islets. Accumulation of ^{111}In-exendin-3 increased with increasing number of islets (100 islets, 39 ± 7.6 amol; 200 islets, 80 ± 1.2 amol; and 400 islets, 112 ± 2.9 amol). The result was an excellent linear correlation between ^{111}In-exendin-3 accumulation and the number of islets ($r = 0.98$, $P = 0.02$). Coincubation with 1 μg (0.2 nmol) of unlabeled exendin-3 blocked the accumulation of ^{111}In-exendin-3 by more than 80% in all conditions, indicating GLP-1R–mediated accumulation.

SPECT/CT Imaging

Islets transplanted into the right calf muscle were clearly visible on SPECT/CT images 4 wk after transplantation, 1 h after injection of ^{111}In-exendin-3 (Fig. 4), with hardly any uptake in the surrounding
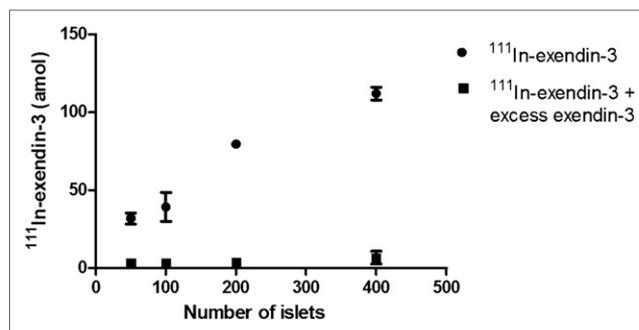

FIGURE 3. Binding of ^{111}In-exendin-3 to 50, 100, 200, and 400 isolated islets of WAG/Rij rats after 4-h incubation at 37°C. ● = total specific binding to isolated islets; ■ = nonspecific binding as determined by coincubation with an excess of unlabeled exendin-3. Data are mean ± SD ($n = 3$/condition).
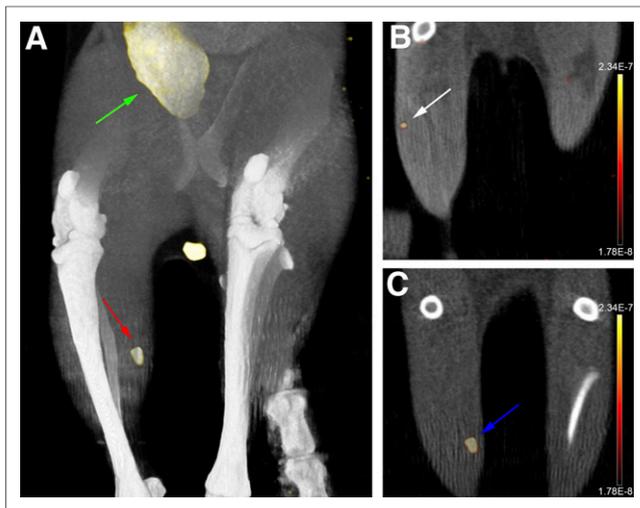
FIGURE 4. (A) Maximum-intensity-projection SPECT/CT image of islets transplanted into right calf muscle of rat (red arrow). Images were acquired 1 h after injection of 15 MBq of ^{111}In-exendin-3. Besides signal from transplant, radioactivity was observed in bladder (green arrow). A clear difference in SPECT signal was observed between rats transplanted with 400 islets (white arrow, B) and rats transplanted with 800 islets (blue arrow, C) (coronal slices).

muscle tissue. Besides accumulation in the transplant, signal was also observed in the bladder (Fig. 4A), kidneys, and lungs. Furthermore, a clear difference in SPECT signal was observed between rats receiving 400 islets ($n = 4$) and rats receiving 800 islets ($n = 5$) (Figs. 4B and 4C). Three animals were excluded from the analysis because no transplant was found immunohistochemically. Uptake in the group with 800 islets was 177 ± 59 Bq (signal-to-noise ratio, 13 ± 3.5), and uptake in the group with 400 islets was 104 ± 4.5 Bq (Fig. 5B) ($P < 0.05$), with a signal-to-noise ratio of 8.8 ± 1.0. On average, the SPECT signal was 1.70 ± 0.44 times higher in the 800-islet group than in the 400-islet group. All SPECT images were fused with CT images for anatomic reference.

Biodistribution

The biodistribution results are summarized in Figure 6. ^{111}In-exendin-3 showed low accumulation in blood, heart, spleen, and liver (maximum, 0.1 percentage injected dose [%ID]/g). Uptake was observed in stomach, duodenum, and lungs (0.74 ± 0.45, 0.51 ± 0.32, and 10.0 ± 5.28 %ID/g, respectively), which

corresponds with previous observations (15). Kidney accumulation was high (31.9 ± 11.5 %ID/g) and was not GLP-1R–mediated. No difference in uptake was observed between muscles containing the transplant and control muscles, because of the small size of the transplant compared with muscle tissue (± 2 g).

Immunohistochemical Analysis

Ex vivo autoradiography showed ^{111}In-exendin-3 tracer accumulation in the islets transplanted into muscle (Fig. 7C). Hardly any background activity was observed in muscle. Tracer accumulation showed colocalization with insulin and GLP-1R expression (Figs. 7A–7C). The positive insulin staining indicates viable and insulin-producing β-cells in the transplant. The average transplant volume was $2.02 \pm 0.16 \times 10^5$ μm³ in the group with 400 islets and $4.30 \pm 0.47 \times 10^5$ μm³ in the group with 800 islets (Fig. 5A) ($P < 0.05$). On average, the transplant volume in the 800-islet group was 1.92 ± 0.24 times larger than that in the 400-islet group.

DISCUSSION

The present study demonstrated the feasibility of in vivo, noninvasive visualization of the islets of Langerhans, transplanted into the calf muscle, using SPECT with ^{111}In-exendin-3 as a tracer. Binding of ^{111}In-exendin-3 to isolated islets in vitro showed a linear correlation between uptake and number of islets. Furthermore, differences in the number of transplanted islets could be detected by in vivo SPECT. Therefore, this noninvasive imaging method is suitable for providing real-time information about β-cell mass in the islet transplant.

Targeting GLP-1R specifically expressed on the β-cells of the pancreatic islets offers an attractive alternative to methods using islets prelabeled with ultrasmall superparamagnetic iron oxide particles as described by Evgenov et al. (7) and others (6,16–18). Targeting a receptor, such as GLP-1R, may potentially offer higher specificity and does not require prelabeling of islets. Furthermore, radiotracer imaging allows quantification of tracer uptake.

It has previously been demonstrated that targeting of GLP-1R with radiolabeled exendin is an elegant method for imaging β-cells, mainly in insulinoma models (14,19) and the native pancreas (15). This strategy was applied by Wu et al., who used PET after injection of exendin-4 labeled with ^{64}Cu or ^{18}F to visualize islets transplanted into the liver (9,20). In these studies, nonspecific uptake of the tracer in the liver caused relatively high background signal (20), which might hamper accurate quantification of GLP-1R–mediated accumulation of the tracer.

We believe that the transplantation model described here may offer significant advantages for determining the number of viable islets in the transplant, for two reasons: first, the complete transplant can be visualized in the muscle with low background signal, and second, the complete transplant can be evaluated immunohistologically because of focal localization of the islets in a predefined area of the calf muscle. Another commonly used focal islet transplantation site in the preclinical setting is the kidney capsule; however, this transplantation site is less suitable than muscle when radiotracers are used, because of their often high kidney uptake (31.9 ± 11.5 %ID/g for exendin).
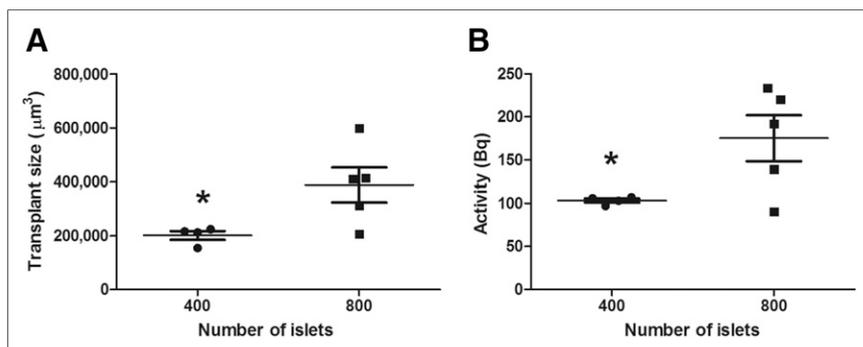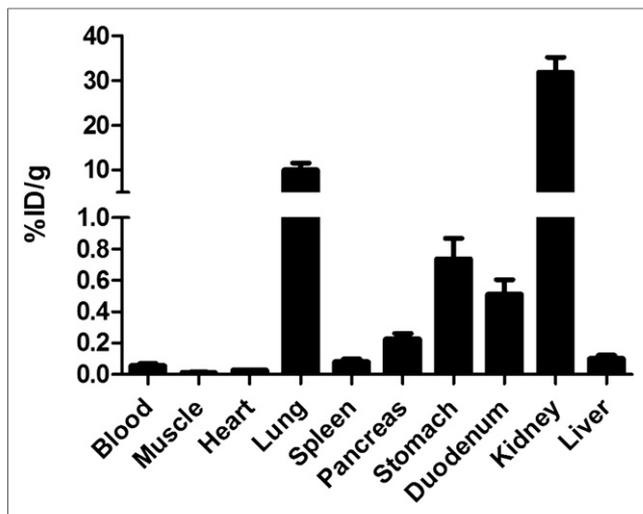

FIGURE 5. (A) Average transplant size based on histology of animals transplanted with 400 or 800 islets ($P < 0.05$). (B) Average SPECT signal of animals transplanted with 400 or 800 islets ($P < 0.05$).

FIGURE 6. Biodistribution of ^{111}In-exendin-3 in WAG/Rij rats ($n = 12$). Values are expressed as %ID/g ± SD. Rats were dissected 2 h after injection.

SPECT/CT images showed clear uptake of the radiolabeled exendin-3, with an average signal-to-noise ratio of 13 ± 3.5 after transplantation of only 800 islets. Furthermore, a difference in SPECT signal between 400 and 800 islets was observed, with the signal of 800 islets being 1.70 ± 0.44-fold higher than that of 400 islets. On the basis of histologic analysis, a 1.92 ± 0.24-fold difference in transplant volume between the 400- and 800-islet groups was observed. This difference between the imaging and histologic data might be explained by the partial-volume effect. The transplant volume was small compared with the resolution of the SPECT system. This factor, in combination with the low uptake, might result in a difference between actual and quantified signal in the transplant. Considering that 400 islets are not sufficient to restore normoglycemia in a clinical setting, this method shows great promise for detecting even small numbers of islets, thus allowing detection of small changes in β-cell mass due to rejection or recurrent autoimmunity. Because of low uptake of our tracer in the liver (0.1 %ID/g), this tracer might also be suited to following islets transplanted into the liver. However, dispersion of the islets throughout the organ might impair the detection capacity of this tracer, and histologic evaluation of the islet transplant size in the liver is highly challenging.

Immunohistochemical analysis of the transplants showed excellent colocalization of the tracer (as determined with autoradiography), insulin, and GLP-1R staining. These findings,
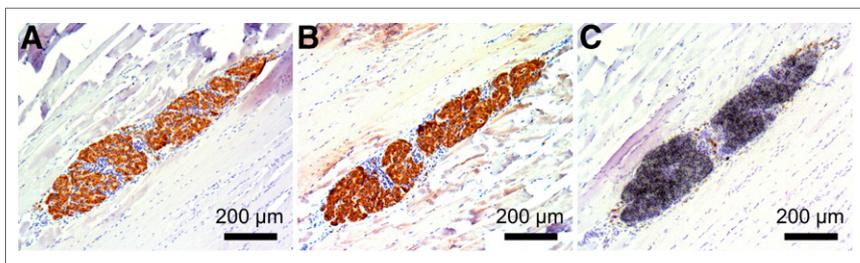
combined with the results for in vitro accumulation of the tracer, demonstrate specific binding of the tracer to the β-cells in the transplanted islets. Moreover, these histologic findings confirm insulin production of the transplanted islets 4 wk after transplantation.

To validate this method for longitudinal imaging of islet transplants, further evaluation of the correlation of tracer uptake in islet transplants of different sizes over time should be considered. Because this tracer is already being used in clinical trials (15), this application can easily be translated and would have the potential to longitudinally measure the effect of therapeutic interventions on the islet mass.

CONCLUSION

In this study, islets transplanted into the muscle of rats were visualized using ^{111}In-exendin-3. Both in vitro and histologic data support specific tracer uptake, and we propose the muscle transplantation model as a highly suitable controlled model for validation of this imaging technology. In vitro, a linear relation between the number of islets and exendin uptake was observed. Furthermore, a significant difference in uptake between 400 and 800 islets was observed in vivo. Because the radiotracer can be injected repeatedly, this method will allow longitudinal monitoring of islet mass in vivo, and because the tracer molecule is already under clinical evaluation (15), clinical studies in patients transplanted with islets appear to be feasible.

DISCLOSURE

REFERENCES

1. Ryan EA, Paty BW, Senior PA, et al. Five-year follow-up after clinical islet transplantation. *Diabetes.* 2005;54:2060–2069.
2. Shapiro AM, Lakey JR, Ryan EA, et al. Islet transplantation in seven patients with type 1 diabetes mellitus using a glucocorticoid-free immunosuppressive regimen. *N Engl J Med.* 2000;343:230–238.
3. Shapiro AM, Ricordi C, Hering BJ, et al. International trial of the Edmonton protocol for islet transplantation. *N Engl J Med.* 2006;355:1318–1330.
4. Lu Y, Dang H, Middleton B, et al. Bioluminescent monitoring of islet graft survival after transplantation. *Mol Ther.* 2004;9:428–435.
5. Chen X, Zhang X, Larson CS, Baker MS, Kaufman DB. In vivo bioluminescence imaging of transplanted islets and early detection of graft rejection. *Transplantation.* 2006;81:1421–1427.

FIGURE 7. ^{111}In-exendin-3 localized in transplanted islets and colocalized with antiinsulin and GLP-1R staining: insulin staining (A), GLP-1R staining (B), and microautoradiography of transplant (C).

6. Jirák D, Kriz J, Herynek V, et al. MRI of transplanted pancreatic islets. *Magn Reson Med.* 2004;52:1228–1233.

7. Evgenov NV, Medarova Z, Dai G, Bonner-Weir S, Moore A. In vivo imaging of islet transplantation. *Nat Med.* 2006;12:144–148.

8. Brom M, Andralojc K, Oyen WJ, Boerman OC, Gotthardt M. Development of radiotracers for the determination of the beta-cell mass in vivo. *Curr Pharm Des.* 2010;16:1561–1567.

9. Wu Z, Liu S, Hassink M, et al. Development and evaluation of ^{18}F-TTCO-Cys40-exendin-4: a PET probe for imaging transplanted islets. *J Nucl Med.* 2013;54:244–251.

10. Christoffersson G, Henriksnas J, Johansson L, et al. Clinical and experimental pancreatic islet transplantation to striated muscle: establishment of a vascular system similar to that in native islets. *Diabetes.* 2010;59:2569–2578.

11. Rafael E, Tibell A, Ryden M, et al. Intramuscular autotransplantation of pancreatic islets in a 7-year-old child: a 2-year follow-up. *Am J Transplant.* 2008; 8:458–462.

12. Stegall MD. Monitoring human islet allografts using a forearm biopsy site. *Ann Transplant.* 1997;2:8–11.

13. Pattou F, Kerr-Conte J, Wild D. GLP-1-receptor scanning for imaging of human beta cells transplanted in muscle. *N Engl J Med.* 2010;363:1289–1290.

14. Brom M, Joosten L, Oyen WJ, Gotthardt M, Boerman OC. Radiolabelled GLP-1 analogues for in vivo targeting of insulinomas. *Contrast Media Mol Imaging.* 2012;7:160–166.

15. Brom M, Woliner-van der Weg W, Joosten L, et al. Non-invasive quantification of the beta cell mass by SPECT with ^{111}In-labelled exendin. *Diabetologia.* 2014;57:950–959.

16. Berkova Z, Kriz J, Girman P, et al. Vitality of pancreatic islets labeled for magnetic resonance imaging with iron particles. *Transplant Proc.* 2005;37: 3496–3498.

17. Tai JH, Foster P, Rosales A, et al. Imaging islets labeled with magnetic nanoparticles at 1.5 Tesla. *Diabetes.* 2006;55:2931–2938.

18. Koblas T, Girman P, Berkova Z, et al. Magnetic resonance imaging of intrahepatically transplanted islets using paramagnetic beads. *Transplant Proc.* 2005;37:3493–3495.

19. Wu H, Liang S, Liu S, Pan Y, Cheng D, Zhang Y. ^{18}F-radiolabeled GLP-1 analog exendin-4 for PET/CT imaging of insulinoma in small animals. *Nucl Med Commun.* 2013;34:701–708.

20. Wu Z, Todorov I, Li L, et al. In vivo imaging of transplanted islets with ^{64}Cu-DO3A-VS-Cys40-exendin-4 by targeting GLP-1 receptor. *Bioconjug Chem.* 2011;22:1587–1594.

Erratum

In Table 2 of the article "Biodistribution and Radiation Dosimetry of the Synthetic Nonmetabolized Amino Acid Analogue *Anti*-^{18}F-FACBC in Humans," by Nye et al. (*J Nucl Med.* 2007;48:1017–1020), certain units of measurement in the column headers are incorrect. The corrected table appears in full below. The authors regret the error.

TABLE 2
Mean Radiation-Absorbed Dose Estimates for *Anti*-^{18}F-FACBC Obtained from MIRDOSE Adult Model

Organ	μGy/MBq	mrad/mCi	μSv/MBq	mrem/mCi
Liver	52.2	193.0		
Pancreas	31.5	116.0		
Heart wall	22.3	82.3		
Kidneys	22.1	81.8		
Spleen	20.2	74.9		
Gallbladder	17.8	66.0		
Red marrow	15.4	56.8		
Adrenals	14.8	54.8		
Muscle	14.7	54.2		
Stomach	13.0	48.1		
Bone surfaces	12.9	47.7		
Urinary bladder wall	11.9	44.2		
Upper large intestine	11.8	43.5		
Lungs	11.7	43.4		
Ovaries	11.6	43.0		
Uterus	11.5	42.5		
Small intestine	11.4	42.2		
Lower large intestine	10.9	40.3		
Thymus	10.0	37.0		
Thyroid	9.4	34.9		
Testes	8.6	31.9		
Brain	8.2	30.4		
Skin	7.0	25.7		
Breasts	4.4	16.1		
Total body	12.8	47.4		
Effective dose equivalent			16.4	60.6
Effective dose			14.1	52.2

Organs are listed in descending order.

The Journal of NUCLEAR MEDICINE

Noninvasive Imaging of Islet Transplants with ^{111}In-Exendin-3 SPECT/CT

Inge van der Kroon, Karolina Andralojc, Stefanie M.A. Willekens, Desirée Bos, Lieke Joosten, Otto C. Boerman, Maarten Brom and Martin Gotthardt

This article and updated information are available at:
http://jnm.snmjournals.org/content/57/5/799

Information about reproducing figures, tables, or other portions of this article can be found online at:
http://jnm.snmjournals.org/site/misc/permission.xhtml

Information about subscriptions to JNM can be found at:
http://jnm.snmjournals.org/site/subscriptions/online.xhtml

SOCIETY OF
NUCLEAR MEDICINE
AND MOLECULAR IMAGING